Simultaneous Measurement of Spectroscopic and Physiological Signals from a Planar Bilayer System: Detecting Voltage-Dependent Movement of a Membrane-Incorporated Peptide†

Yoshiro Hanyu,* Toru Yamada, and Gen Matsumoto‡

Biophysics Section, Electrotechnical Laboratory, 1-1-4 Umezono, Tsukuba, Ibaraki, 305-8568, Japan

Received May 1, 1998; Revised Manuscript Received August 27, 1998

ABSTRACT: We developed an experimental system that can measure spectroscopic and physiological signals simultaneously from ion channels in a planar lipid bilayer, to study the relationship between the structure and function of the ion channels. While the membrane potential was clamped, fluorescent emission and ionic currents were measured simultaneously. The fluorescent emissions from a planar bilayer constructed in a specially designed chamber were monitored exclusively, and the signal intensity was measured with a photon-counting system. The intensity of fluorescence and spectral shape were measured successfully from the planar bilayer, with a high signal-to-noise ratio. The system can measure the intensity of fluorescence from a restricted area of the planar bilayer, with a diameter of 70 μm and a focal depth of 15 μm. The low background signal was achieved by optimizing the optical system. More than 95% of the measured fluorescence comes from the planar lipid bilayer. A 22-mer peptide with a sequence identical to that of the S4 segment of the electric eel sodium channel domain IV was synthesized and fluorescence-labeled. This peptide formed a voltage-dependent ion channel in a planar bilayer. The changes in the intensity of the fluorescence accompanying ionic currents generated by a voltage clamp suggest that voltage gating involves the insertion of the N-terminal of the peptide into the membrane. The electrical and optical signals were measured with a gate time of 10 ms. This measurement enabled the detection of movement of the membrane-incorporated peptides with channel opening.

Detailed knowledge of the structure and dynamics of membrane-associated proteins and peptides is essential for understanding their function and interactions with membrane lipids. Since it is particularly difficult to determine the structure of membrane-associated proteins, very little is known about their 3-D structures. Furthermore, technical problems make it difficult to study the conformational changes that are directly related to the function of proteins. It is therefore very important to study the structure and function of membrane-associated proteins simultaneously, to elucidate the structural changes in functioning membrane-associated proteins. The structure and function of channel-forming peptides and proteins were studied in different systems. The functions of channel-forming peptides, such as their activation curve and ionic selectivity, were studied in detail electrophysiologically, using a planar bilayer system. Studies of several natural peptides including alamethicin (*1*) and melittin (*2*) have shown that small, amphiphilic α-helixes might aggregate to form ion channels in the membrane. Synthetic peptides have also been employed as a model system to learn more about the structure−function relationship of ion channels. A 21-residue model peptide containing only leucine and serine residues formed ion channels (*3*). It was also found that the peptides with sequences corresponding to putative transmembranous domains and pore-lining regions deduced from the primary structures of various kinds of channels formed voltage-dependent channels in planar lipid bilayers (*4*−*7*). The conformation of these natural and synthetic channel-forming peptides in membranes has also been studied spectroscopically. A spectrofluorimetric approach identified the orientation of melittin (*8*), the orientation and aggregation of Magainin 2 (*9*), the transmembranal localization of the sodium channel S4 segment (*10*), and the organization of the α5 and α7 helices of δ-endotoxin (*11*). The S4−S45 segment of the voltage-sensitive sodium channel shows polarity-dependent conformational switching (*12*). These approaches to inferring structural information about ion channels are very important, since technical limitations prevent full elucidation of the 3-D structure of the channels.

The experiments referred to above considered the structure and function of channel-forming peptides separately; structure was studied in a liposome system and function was studied in a planar lipid bilayer system. In the liposome system, the functional state of the channels is not properly controlled. On the other hand, the planar lipid bilayer system is good for studying the function of ion channels, but it yields little information on their structure. To detect the structural changes involved in gating, precise spatio-temporal control of the functional state is necessary while studying the changes in structure. Thus, both the function and the structure of an

† This work was supported by PRESTO program from Japan Science and Technology Corporation.

* To whom correspondence should be addressed. Tel: +81-298-54-5542. Fax: +81-298-54-5540. E-mail: hanyu@etl.go.jp.

‡Present address: Brain Science Institute, The Institute of physical and chemical research (RIKEN) Wako, Saitama 351-01, Japan.

10.1021/bi981003f CCC: $15.00
Published on Web 10/16/1998

ion channel in a planar bilayer membrane must be measured simultaneously, while the functional state of the channel is properly controlled. The transmembranous movement of the channel-forming domain in colicin Ia was previously detected by mapping the topology of the channel-forming domain with respect to a planar membrane (*13*). However, to determine the structure with a high temporal resolution, optical methods should be employed. Some studies recording optical signals from a planar lipid bilayer have been reported (*14*, *15*). In this paper, we present the first system designed to optically record ion channel gating in a planar lipid bilayer. We have developed an experimental system that can measure the ionic current (function) and fluorescence emission (structural change) of an ion channel in an artificial planar lipid bilayer, while controlling the membrane potential. In this study, a 22-mer peptide with a sequence identical to that of the S4 segment of the electric eel sodium channel domain IV was used as a model amphiphilic helix that can form ion channels. A fluorescence-labeled S4 peptide was synthesized and incorporated into the bilayer. Structural changes in the S4 peptide were observed while precisely controlling its functional state. This study is the first to present results on the movement of functioning channel-forming peptides in a planar lipid bilayer.

EXPERIMENTAL PROCEDURES

Materials. Asolectin was purchased from Associated Concentrates Inc. (Woodside, NY) and purified by acetone precipitation and ether extraction as described (*16*). TRITC DHPE[1] was purchased from Molecular Probes (Eugene, OR). 5-SLPC was purchased from Avanti Polar Lipids Inc. (Alabaster, AL).

Peptide Synthesis and Purification. A 22-mer peptide with a sequence identical to that of the S4 segment of the electric eel sodium channel domain IV (*17*) was synthesized by a solid-phase method. This peptide has the following structure: Arg-Val-Ile-Arg-Leu-Ala-Arg-Ile-Ala-Arg-Val-Leu-Arg-Leu-Ile-Arg-Ala-Ala-Lys-Gly-Ile-Arg. Its N-terminal was labeled with tetramethyl rhodamine isothiocyanate (Molecular Probes, Eugene, OR). The rhodamine-labeled S4 peptide of the sodium channel was denoted R-S4. The synthetic peptide was purified to 95% chromatographic homogeneity by reverse-phase HPLC in a C18 column (Beckman Instruments Inc., Fullerton, CA) using a linear gradient of 20%−50% acetonitrile in 0.1% trifluoroacetic acid for 25 min. The peptide was subjected to mass spectroscopic analysis to confirm its composition.

Planar Lipid Bilayer Formation. A specially designed chamber was used for the simultaneous electrical and optical measurements (Figure 1). The chamber consists of two blocks of PTFE and PTFE film with a cover glass for the optical windows. A piece of PTFE film (Nichiryo, Japan) 25 μm thick, with a hole 120 μm in diameter (made by an electric arc), was clamped in the chamber so that the hole was in the center. The chambers on each side of the hole were pretreated with 0.5 μL of 1% *n*-hexadecane in hexane.

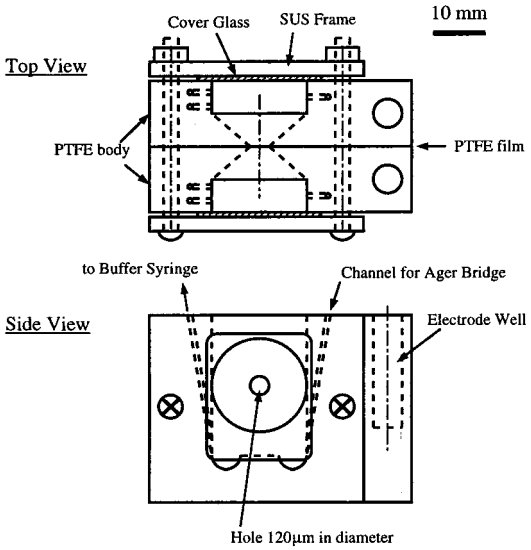

FIGURE 1: Top and side views of the bilayer membrane chamber used for the simultaneous electrical and optical measurements.

To form a folded bilayer (*18*), buffer was added to each side of the chamber so that the level was below the hole in the PTFE film. A solution of lipid in hexane (5 mg/mL) was spread on top of the buffer solution and left for a few minutes to allow the hexane to evaporate. The buffer level in both compartments was raised to form a planar lipid bilayer. The formation of the bilayer was monitored by capacitance measurements. Peptide was added to the cis side of the chamber, with stirring. When fluorescence-labeled lipids and spin-labeled lipids were used, they were first mixed with an asolectin solution in hexane before being applied to the top of the buffer solution.

Ionic Current Measurements. Electrical measurements were made with an Axopatch200A (Axon Instruments Inc., Foster City, CA) using the chamber described above. The command voltage was generated by the program pClamp (version 5.5.2 Axon Instruments Inc.). The voltage was applied through an agar bridge and a Ag/AgCl electrode on the cis side of the cell, the side to which the peptides were added. The trans side was virtually grounded through an agar bridge and a Ag/AgCl electrode. The current flowing through the bilayer was recorded and analyzed with pClamp.

Fluorescence Measurements From the Planar Bilayer. The fluorescent emissions from the planar lipid bilayer were measured in the newly developed experimental system using the chamber described above. A schematic diagram of the experimental system is shown in Figure 2. The excitation light was focused on the planar lipid bilayer with an objective lens (Olympus UPlanFl/4 N/A = 0.13, Japan). The optical system was adjusted so that only an area of the planar bilayer with a diameter of 80 μm was irradiated. This was achieved by monitoring the focused beam on the planar bilayer directly with a CCD camera. The fluorescent emissions were collected through the objective lens and sent to the photomultiplier (R643S, Hamamatsu Photonics, Japan). Any fluorescence from other areas was blocked by pinholes placed after the objective lens. Scattered light was eliminated by a dichroic mirror and two long-pass glass filters (RG560). The intensity of fluorescence was measured by photon-counting methods (PC-545AS, NF Electrics Inc., Japan). The emission spectrum was measured with a multichannel analyzer

[1] Abbreviations: TRITC DHPE, *N*-6(6-tetramethylrhodaminethiocarbamoyl)1,2-dihexadecananoyl-*sn*-glycero-3-phosphoethanolamine triethylammonium salt; 5-SLPC, 1-palmitoyl-2-stearoyl(5-DOXYL)-*sn*-glycero-3-phosphocholine; HPLC, high-performance liquid chromatography; PTFE, poly(tetrafluoroethylene).

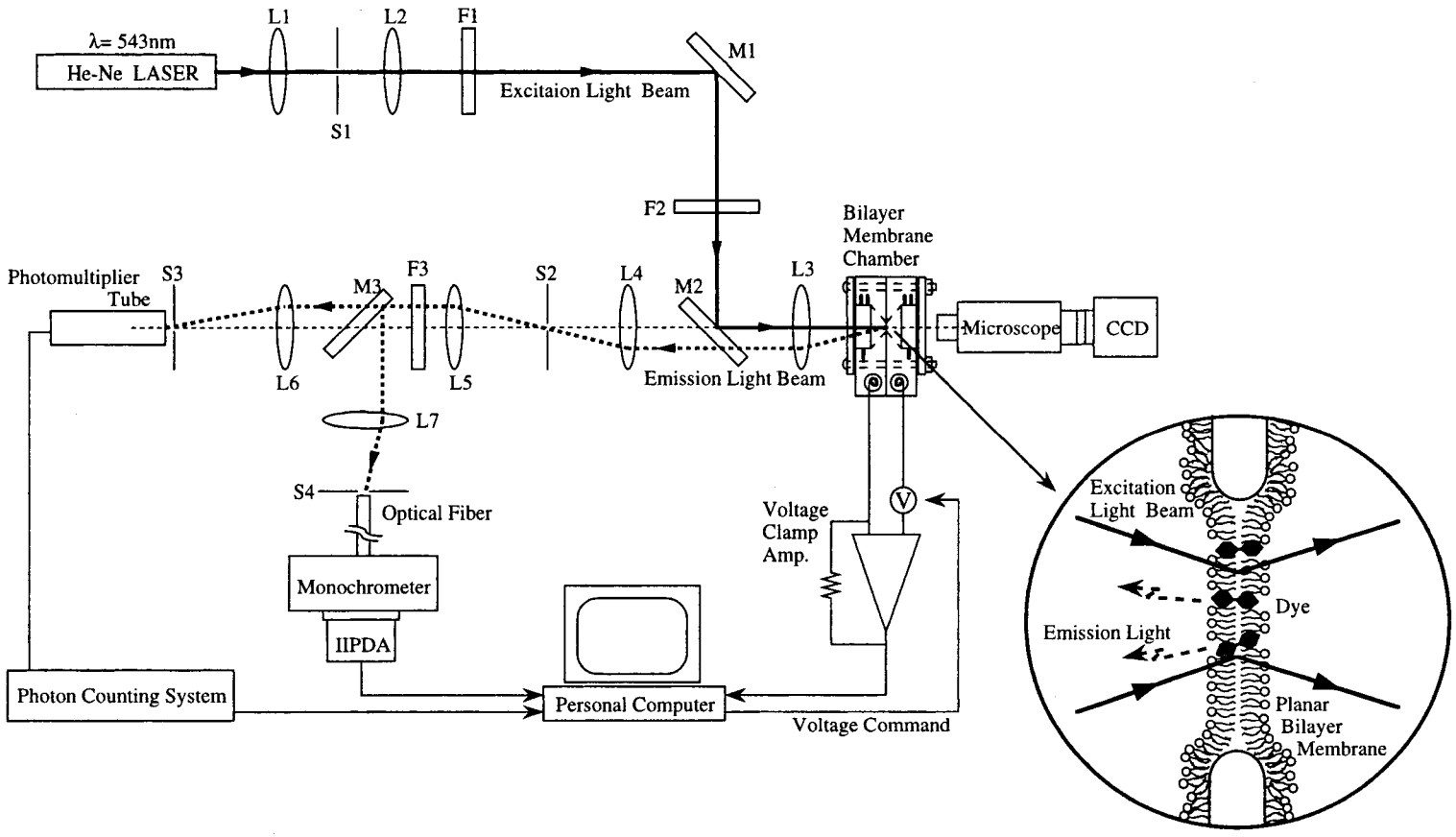

FIGURE 2: A schematic diagram of the experimental system: L1-L7, lenses; F1, ND filter; F2, band-pass filter (λ = 543 nm); F3, long-pass glass filter (RG560); M1, plane mirror; M2, dichroic mirror (λ = 560 nm); M3, beam splitter; S1−S4, pinhole slits. Excitation light from a He−Ne laser was filtered with F1 and F2, and then reflected by a dichroic mirror M2 and focused with an objective lens L3 (N/A = 0.13). The focal point was monitored with a microscope and a CCD camera (×40). The restricted area of the folded membrane in the bilayer membrane chamber was positioned in the focal point. The backward emitted florescence was collected with lens L3 and was filtered with F3. M3 split the emission beam into two beams, which go to the photon-counting system and the multichannel spectrum analyzer.

(IRY-700, Princeton Instruments Inc., NJ). The data were stored in and analyzed with a PC compatible computer.

RESULTS

Measuring Fluorescence from a Planar Bilayer. The fluorescent emissions from a TRITC DHPE containing planar lipid bilayer were measured. The spectra are shown in Figure 3A. The fluorescent emissions were observed around 590 nm using a single 560-nm long-pass filter in the emission light-collecting path. Scattered light from the excitation laser beam appeared as a sharp line at 543 nm. Two 560-nm long-pass filters eliminated almost all of the scattered light, while conserving the shape of the fluorescence spectrum. Therefore, this system was able to measure fluorescent emission exclusively. The background level of the signals was checked in the following manner: The membrane was ruptured by applying 1.3 V for 1 ms. When the membrane ruptured, the conductance became very large and therefore the current was overloaded. When this happened, the intensity of fluorescence decreased quickly to less than 5% of the original value, as shown in Figure 3B. This shows that more than 95% of the measured fluorescence comes from the planar lipid bilayer. The low background signal was achieved by optimizing the optical system. The diameters of the pinholes in the excitation light pathway were adjusted so that the diameter of the area of the planar membrane irradiated was 70 μm. The diameters of the pinholes in the emission light pathway were also adjusted so that only emission light from the irradiated area was detected. Thus, the optical components were adjusted to work confocally. No photobleaching was observed with the intensity of excitation used in the experiment.

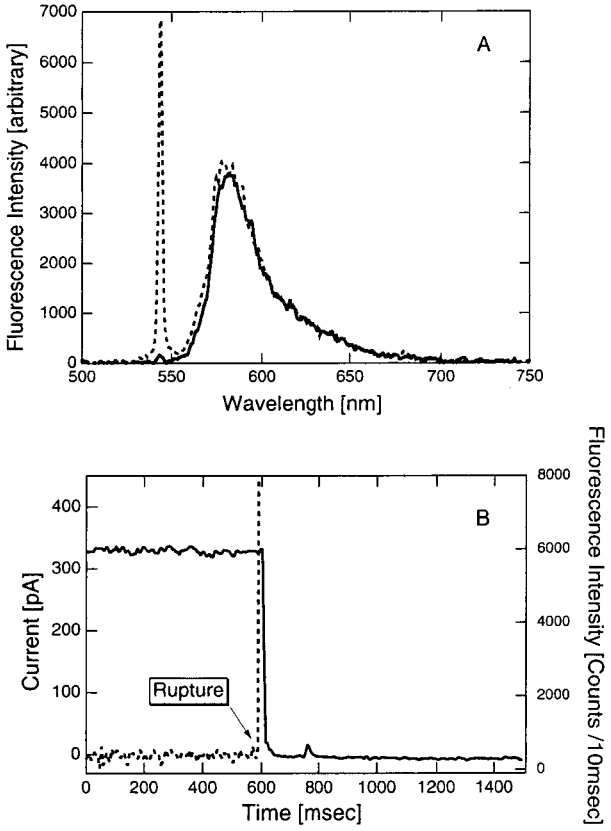

FIGURE 3: Fluorescent emission from a planar lipid bilayer containing TRITC DHPE. Lipids: Asolectin was added to the cis side, and a mixture of asolectin−TRITC DHPE 100:1 was added to the trans side. The buffer solution on both sides was 100 mM sodium chloride and 50 mM Tris buffer (pH = 7.5). (A) Emission spectrum from the planar lipid bilayer containing TRITC DHPE. Emission spectra through one and two 560-nm long-pass glass filters are shown in dashed and solid lines, respectively. The exposure time for the multichannel spectrum analyzer was 1 s. (B) Change in the intensity of fluorescence after rupturing the membrane. A voltage pulse of 1.3 V was applied to the membrane for 1 ms. The intensity of fluorescence was monitored by the photon-counting method with a gate time of 10 ms. The electric current and intensity of fluorescence are shown with dashed and solid lines, respectively.

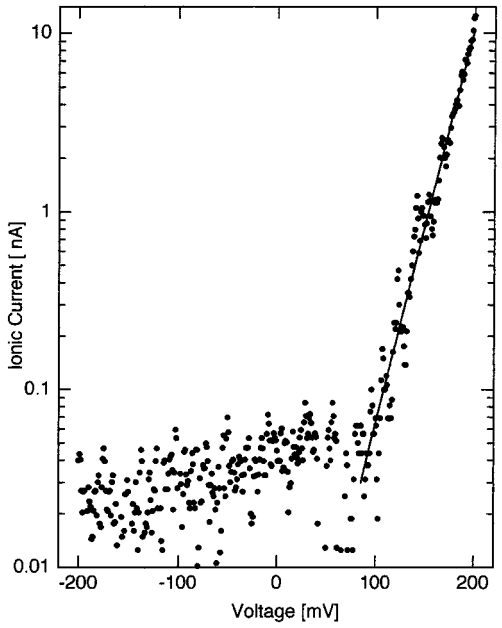

FIGURE 4: Current−voltage (I−V) relationship for R-S4 at a concentration of 500 nM on the cis side of the buffer solution. R-S4 was added to the cis side after formation of an asolectin bilayer with stirring. The buffer solution on the cis side was 1 M sodium chloride and 50 mM Tris buffer (pH = 7.5). To remove unbound R-S4, the cis side was perfused with 3 volumes of buffer. A ramp voltage command (1 mV/s) was applied to the membrane to measure the I−V relationship. The voltage-dependent current (I) could be fitted with the following exponential relationship: $I = I_0 \exp(V/\mathrm{Ve})$, where Ve is 19.6 mV.

Formation of Voltage-Dependent Ion Channel by R-S4. The current−voltage relationship (I−V curve) shown in Figure 4 was obtained with a ramp voltage clamp after adding the rhodamine-labeled S4 peptide (R-S4) and perfusing the solution. The relationship was independent of the ramp speed applied in the range from 0.5 mV/s to 10 mV/s. As shown in Figure 4, R-S4 formed a voltage-dependent ion channel. Ionic current was only generated with deporalization. The dependence of current on voltage above 100 mV could be fitted by an exponential relationship:

$$I = I_0 \exp(V/\mathrm{Ve})$$

where Ve is measured as 19.6 mV. The current−voltage relationship was monitored with ramps until a stable relationship was obtained. It took about 10 min to reach a steady current−voltage state. The conductance was increased until the steady state was reached. This increase in conductance was not due to the binding of aqueous R-S4 to the membrane, because the unbound soluble R-S4 was quickly removed after the addition of R-S4 by perfusion.

Movement of R-S4 with Voltage Gating. Changes in the intensity of the fluorescence of R-S4 in a planar membrane

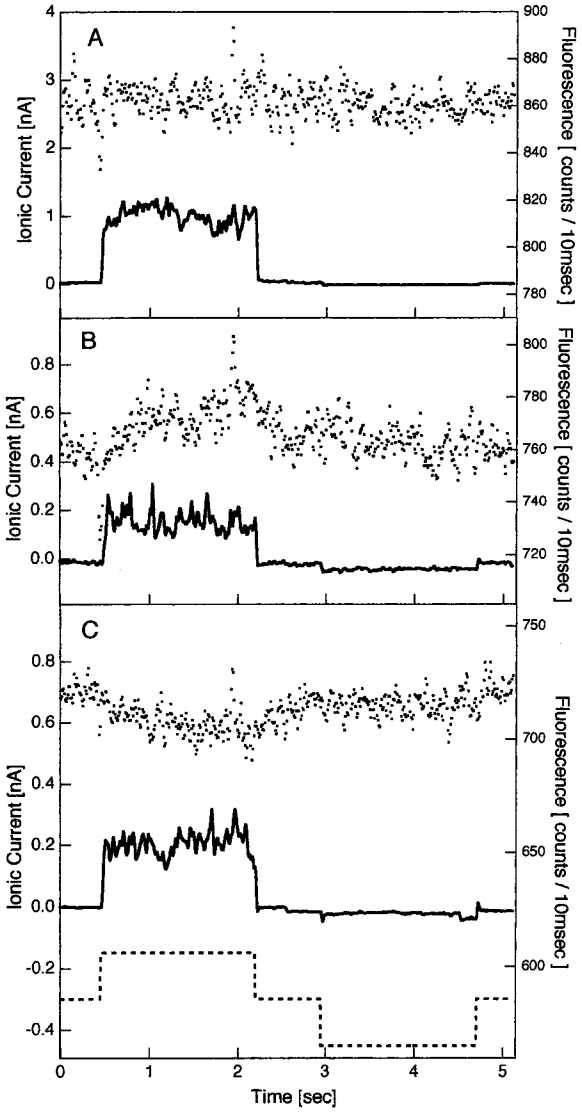

FIGURE 5: Simultaneous measurements of ionic current and the intensity of fluorescence with voltage clamp. A rectangular depolarizing or hyperpolarizing command voltage, ±150 (mV) with a duration of 1.75 s was applied to the planar bilayer. Fluorescence intensity was monitored using photon-counting methods with a gate time of 10 ms. The intensity of excitation was adjusted so that the intensity of emission was about 800 counts/10 ms. The aqueous concentration of R-S4 in the cis side was 500 nM. To remove unbound R-S4, the cis side was perfused with 3 times the volume of buffer: (A) 1 M sodium chloride on both sides of the chamber; (B) 0.5 M potassium iodine and 50 mM sodium chloride on both sides of the chamber; and (C) 10 mol % 5-SLPC in the trans side of the membrane, and 1 M sodium chloride on both sides of the chamber. In all cases, 50 mM Tris buffer (pH = 7.5) was used; solid lines, ionic current (nA); dots, intensity of fluorescence (counts/10 ms); dashed lines, command voltage ±150 (mV).

due to voltage gating were measured. When a steady current−voltage state had been reached, a rectangular depolarizing or hyperpolarizing command voltage with a duration of 1.75 s was applied to the planar bilayer. The drift of the intensity of fluorescence was less than 20 counts/10 ms per min with each experiment. The fluorescent emissions and ionic current were measured simultaneously (Figure 5). The mean values of the intensity of fluorescence and the current during the command were calculated and compared with those from the resting state ($V = 0$ mV) are shown in Table 1. As a control experiment, 1 M NaCl was added to both sides of the chamber (Figure 5A). In this case, the relative changes in the intensity of fluorescence following hyperpolarizing and depolarizing voltages were smaller than 0.2%, which is within the statistical deviation. To study the changes in the environment surrounding R-S4, fluorescence-quenching agents were added to the chamber. When the quenching agent was added, a significant change in the intensity of fluorescence was detected with the application of a depolarizing voltage that generated an ionic current. When the aqueous quencher potassium iodide was added, the intensity of fluorescence increased by 0.98% at the depolarizing voltage (Figure 5B). When the membrane quencher was on the trans side of the bilayer membrane (5-SLPC), the intensity of fluorescence decreased by 1.22% at the depolarizing voltage (Figure 5C). However, at the hyperpolarizing voltage, which does not generate an ionic current, no changes in the intensity of fluorescence were observed when the fluorescence quencher was used on either side of the membrane. These results show that the fluorophore of the N-terminal of S4 migrates into the membrane when the channel opens with depolarization and generates an ionic current. The background fluorescence was measured after each experiment by rupturing the membrane. It was smaller than 5% each time.

Table 1: Changes of Ionic Current and Fluorescence Intensity with Voltage Gating[a]

environment	command voltage (mV)	fluorescence (count/10 ms)	ΔF (%)	ionic current (pA)
NaCl	0	861.7 ± 1.6		0.0 ± 2.1
(control)	+150	863.0 ± 1.5	0.15 ± 0.25	982.6 ± 23.3
	−150	860.3 ± 1.4	−0.16 ± 0.25	−35.9 ± 0.5
KI	0	763.5 ± 1.4		0.0 ± 3.6
	+150	771.0 ± 1.4	0.98 ± 0.26	163.3 ± 9.9
	−150	763.4 ± 1.3	−0.015 ± 0.25	−30.3 ± 1.1
5-SLPC	0	717.1 ± 1.5		0.0 ± 2.8
	+150	708.3 ± 1.2	−1.22 ± 0.27	201.9 ± 7.4
	−150	714.9 ± 1.2	−0.31 ± 0.27	−18.9 ± 1.0

[a] The data of the intensity of fluorescence and the current in Figure 5A−C were averaged during the command. ΔF is the relative change of the intensities of fluorescence at the command which was normalized with those from the resting state ($V = 0$ mV).

DISCUSSION

To study the structural change of active ion channels, we developed an experimental system that can measure both optical and electrical signals simultaneously from channels reconstituted in a planar lipid bilayer. The intensity of fluorescence and spectral shape from a planar bilayer were measured successfully, with a high signal-to-noise ratio. The system can measure the intensity of fluorescence from a restricted area of the planar bilayer, with a diameter of 70 μm and a focal depth of 15 μm. We used an objective lens with a relatively small numerical aperture (N/A = 0.13), so that any optical aberration produced by the thick layer of water in the chamber would be reduced. The small aperture reduces the optical aberration, but measurement of the fluorescent emissions is poor. If the appropriate compensation for an objective lens with a large aperture was used, the system would be able to measure a larger amount of the fluorescent emission with a higher signal-to-noise ratio, due to the smaller focal depth. The power of the He−Ne laser

(0.75 mW) used as a light source for excitation was attenuated by $10^{-3}-10^{-4}$ with spatial and neutral density filters. At these excitation intensities, nonspecific conductance leaks due to the photodynamic effect (*19*) were not observed. The I−V characteristics of the R-S4 channel did not change according to the presence or absence of excitation irradiation.

A 22-mer peptide with a sequence identical to that of the S4 segment of the electric eel sodium channel domain IV (*17*) was synthesized and fluorescence-labeled. This peptide (R-S4) formed voltage-dependent ion channels in a planar bilayer. The dependence of current on voltage was well fitted by an exponential relationship. The current for positive voltages increased *e*-fold for every 19.6 mV increase in voltage (above 100 mV). The current−voltage curve was quantitatively different from that of Tosteson et al. (*6*). They reported that the conductance for positive potentials (above 40 mV) increased *e*-fold for every 10 mV increase in potential. These differences may be due to the different lipids used; they used a negatively charged phospholipid, while we used a neutral phospholipid. Brullemans et al. showed that the Ve of the S4−S45 peptide for the negatively charged phospholipid is 9 mV, while that for the neutral phospholipid is 19 mV (*7*).

After binding to the membrane, it took some time for R-S4 to reach a steady current−voltage state. The current was increased at a fixed voltage until the steady state was reached. An increase of ionic current over a similar length of time also occurs with the channel-forming peptide melittin (*20*), although the adsorption of melittin was very quick, on the order of milliseconds (*21*). It has been suggested that this period is necessary for the membrane-adsorbed peptide to rearrange its configuration in the membrane, to form the channel. Brullemans et al. estimated the mean apparent number of monomers per conducting aggregate to be 3−5 (*7*). These results suggest that S4 first binds to the surface of the membrane and then forms an ion channel by forming clusters with other S4 peptides. This clustering takes about 10 min. We measured the intensity of fluorescence from R-S4 during this period. The intensity of fluorescence also increased with time (data not shown). The increase in the intensity of fluorescence means that rhodamine is moving from the surface to the inside of the membrane since the quantum yield of rhodamine is higher inside the membrane. When the intensity of the fluorescence did not change, the I−V curve remained unchanged. This suggests that the clustering occurs when R-S4 penetrates the membrane.

We measured the intensity of fluorescence and the ionic current of R-S4 simultaneously with voltage gating in a planar bilayer. Changes in the intensity of fluorescence of R-S4 in a planar membrane when the command voltage lasted between 100 msec and 10 s were measured. With a duration of 1.75 s, the statistical deviation of the relative changes in the intensity of fluorescence was as small as 0.3%, which was small enough to detect the changes in the intensity of fluorescence due to the voltage gating. With a longer duration, we could measure the smaller changes with better resolution, but lost the temporal resolution. The background fluorescence in these measurements was smaller than 5%, so the observed fluorescence was almost all from the membrane-incorporated R-S4.

To study the changes in the environment surrounding R-S4 with voltage gating, fluorescence quenchers were added to the chamber. Significant changes in the intensity of fluorescence were only detected at the depolarizing voltage that generated an ionic current. When the quencher was in the membrane, the intensity of fluorescence decreased with current generation. The change in the intensity of fluorescence was 1.22% with a lipophilic quencher. The degree of movement can be estimated from the experiment involving depth-dependent fluorescence quenching of a tryptophan residue on the ColicinE1 channel (*22*). In this paper, the authors studied the quenching of tryptophan fluorescence from single-tryptophan mutants of the ColicinE1 channel, using a lipophilic quencher (5-SLPC and 12-SLPC). When 10 mol % SLPC was present in the liposomes, the same amount as in our experiment, the intensity of fluorescence with 5-SLPC was compared with that with 12-SLPC. The intensities of fluorescence were reduced by 4% and 15% for tryptophan 355 and 460, respectively. The difference in the depth of the quenchers between 5-SLPC and 12-SLPC was about 6.5 Å. The intensity of the fluorescence was reduced by approximately 1−2%/Å. The changes that we detected were about 1% at 150 mV. If all the peptides in the membrane formed the voltage-dependent channel, the movement was estimated to be only 1 Å in depth. This value seems to be too small for gating. Most of the fluorescence might come from the membrane-incorporated peptides that do not form voltage-dependent channels. Jhon and Jähnig (*23*) studied the aggregation states of melittin in lipid vesicle membranes with fluorescence energy transfer and revealed that the percentage of aggregated melittin was on the order of 10%. If this is also true in our case, the movement with voltage gating is larger than 1 Å. On the other hand, when the quencher was in the aqueous phase, the intensity of fluorescence increased by 0.98% with current generation. This change can be interpreted as the movement of fluorophores into the interior of the membrane when voltage gating opens a channel. It is not possible to estimate the movements of the peptide quantitatively in this case. However, the opposite sign of the changes with aqueous and lipophilic quenchers revealed that the N-terminal of the S4 peptide moves into the interior of the membrane with voltage gating.

Hellium et al. showed that S4−S45 peptide from the voltage-sensitive sodium channel changes its secondary structure (from a β-sheet to an α-helix) by decreasing the polarity of the solvent (*17*). In this paper, we show that the insertion of a peptide into a membrane with a lower polarity than the outer solution occurs during voltage gating. Combining these results, activation of the channels that are formed by R-S4 occurs when S4 (or S4−S45) peptide moves into the membrane by changing its secondary structure when the depolarizing voltage is applied.

With the experimental system developed in this paper, structural changes of ion channels can be detected with precise spatio-temporal control of their functional state. This method should prove to be a useful tool for elucidating structure−function relationships for other membrane proteins. The signal/noise ratio needs to be improved to detect structural changes more precisely. Larger changes of fluorescence with the movement of the fluorophore are expected when the quencher is located near the fluorophore. In our experiment, the lipophilic quencher was located on

the trans side of the membrane while the peptide was added to the cis side of the chamber. If the fluorophore is located in the cis membrane, the lipophilic quencher should also be on the cis side of the membrane to obtain the larger signals. We could not measure the signals, since the planar lipid bilayer was unstable under these conditions. Other spectroscopic techniques should now be applied for further improvement. By using an environmentally sensitive dye (*10*) instead of rhodamine, changes in the polarity around the fluorophore could be determined more precisely. Also, information on the degree of insertion could be obtained quantitatively using parallax methods (*22*, *24*). Furthermore, to gain insight into the ion channel properties of an intact ion channel, techniques used to introduce a probe into an active channel and to reconstitute the labeled channel in planar bilayers with a proper orientation should be developed.

ACKNOWLEDGMENT

The authors are indebted to Professor F. Oosawa (Aichi Institute of Technology, Toyota, Japan) and Dr. W-S. D. Griggs (John Hopkins University) for stimulating discussion. We wish to thank Professor M. Sokabe (Nagoya University, Nagoya, Japan) and Dr. M. Tsushima (National Institute of Sericultural and Entomological Science, Tsukuba, Japan) for inspiring discussion and for the opportunity to visit their labs while planar lipid bilayers were being prepared.

REFERENCES

1. Hall, J. E., Vodyanoy, I., Balasubramanian, T. M., and Marshall, G. R. (1984) *Biophys. J. 45*, 233−247.
2. Hanke, W., Methfessel, C., Wilmsen, H. U., Katz, E., Jung, G., and Boheim, G. (1983) *Biochem. Biophys. Acta 727*, 108−114.
3. Lear, J. D., Wasserman, Z. R., and DeGrado, W. F. (1988) *Science 240*, 1177−1181.
4. Sthümer, W. (1991) *Annu. Rev. Biophys. Biophys. Chem. 20*, 65−782.
5. Oiki, S., Danho, W., and Montal, M. (1988) *Proc. Natl. Acad. Sci. U.S.A. 85*, 2393−2397.
6. Tosteson, M. T., Auld, D. S., and Tosteson, D. C. (1989) *Proc. Natl. Acad. Sci. U.S.A. 86*, 707−710.
7. Brullemans, M., Helluin, O., Dugast, J.-Y., Molle, G., and Duclohier, H. (1994) *Eur. Biophys. J. 23*, 39−433.
8. Kempf, C., Klausner, R. D., Weinstein, J. N., Renswoude, J. V., Pincus, M., and Blumenthal, R. (1982) *J. Biol. Chem. 257*, 2469−2476.
9. Matsuzaki, K., Murase, O., Tokuda, H., Funakoshi, S., Fujii, N., and Miyajima, K. (1994) *Biochemistry 33*, 3342−3349.
10. Rapaport, D., Danin, M., Gazit, E., and Shai, Y. (1992) *Biochemistry 31*, 8868−8875.
11. Gazit, E., and Shai, Y. (1995) *J. Biol. Chem. 270*, 2571−2578.
12. Helluin, O., Breed, J., and Duclohier, H. (1996) *Biochem. Biophys. Acta 1279*, 1−4.
13. Qiu, X. Q., Jakes, K. S., Kienker, P. K., Finkelstein, A., and Slatin, S. L. (1996) *J. Gen. Phisiol. 107*, 313−328.
14. Dragsten, P. R., and Webb, W. W. (1978) *Biochemistry 17*, 5228−5240.
15. Ladha, S., Mackie, A. R., Harvey, L. J., Clark, D. C., Lea, E. J. A., Brullemans, M., and Duclohier, H. (1996) *Biophys. J. 71*, 1364−1373.
16. Kagawa, Y., and Racker, E. (1971) *J. Biol. Chem. 246*, 5477−5487.
17. Noda, M., Shimizu, S., Tanabe, T., Takai, T., Kayano, T., Ikeda, T., Takahasi, H., Nakayama, H., Kanaoka, Y., Minamino, N., Kanagawa, K., Matsuo, H., Raftery, M. A., Hirose, T., Inayama, S., Hayasida, H., Miyata, T., and Numa, S. (1984) *Nature 312*, 121−127.
18. Montal, M., and Mueller, P. (1972) *Proc. Natl. Acad. Sci. U.S.A. 69*, 3561−3566.
19. Kunz, L., and Stark, G. (1997) *Biochem. Biophys. Acta 1327*, 1−4.
20. Pawlak, M., Stankowski, S., and Schwarz, G. (1991) *Biochem. Biophys. Acta 1062*, 94−102.
21. Schwarz, G., and Beschiaschvili, G. (1989) *Biochem. Biophys. Acta 979*, 82−90.
22. Palmer, L. M., and Merril, A. R. (1994) *J. Biol. Chem. 269*, 4187−4193.
23. Jhon, E., and Jähnig, F. (1991) *Biophys. J. 60*, 319−328.
24. Chattopadhyay, A., and London, E. (1987) *Biochemistry 26*, 39−45.

BI981003F